International Journal of Science and Research (IJSR)
ISSN (Online): 2319-7064
Index Copernicus Value (2015): 78.96 | Impact Factor (2015): 6.391

Fatigue Life Prediction of Structural Metals under Mixed Mode Loading Condition

Saad Sami Al-Khfaji

Ministry of Higher Education & Scientific Research,
Baghdad – Iraq
dr.saad[at]scrdiraq.gov.iq

Abstract: ***In this paper, fatigue life prediction of two types of structural metals, (2024-T4) Al-alloy and (304L) steel alloy under mixed mode loading (prior torsion and cyclic bending) were investigated. The rotating bending fatigue machine (HSM 19) was utilized to implement all the tests which were carried out at laboratory temperature and zero mean stress. Two types of fatigue tests were conducted namely; constant amplitude loading tests leading to constructing the S-N curves with and without prior torsion for the two alloys and variable amplitude loading tests to study the effect of mixed mode loading on cumulative fatigue damage. The second type of tests was conducted according to the (Low-High) test program and block test program. Based on the experimental results, (4) S-N curves were constructed which clearly show the effect of mixed mode on the predicted fatigue life for the two alloys. In addition, the experimental results of mixed mode loading (with prior torsion 20) show that for 2024-T4 Al – alloy fatigue lives increase while for 304L Steel fatigue lives decrease. Moreover, the experimental results for cumulative fatigue damage were safe and agree with Miner rule.***

Keywords: Fatigue failure, fatigue life, mixed mode, metal fatigue**.**

1. Introduction

Fatigue life prediction for structural metals is a vital engineering problem. Fatigue designers are essentially interested in obtaining an accurate prediction for fatigue life of mechanical components subjected to dynamic loads to avoid sudden failure which usually results in a serious disasters if happens in airplanes or trains parts. Fatigue life estimation of a part or a structure is generally provided from experimental tests for specimens of that metal subjected to same loading to enable constructing fatigue life curve, number of cycles till to failure. This curve is obtained by testing specimens under constant amplitude loads. Fatigue failure can be described as the process of crack initiation and growing to reach till to critical volume which will consequently leads to sudden failure in the mechanical components as a result of subjecting to the reverse cyclic stresses [1]. Three main factors play a significant role in fatigue failure. These are; crack length, cycle stress and environmental condition [2]. The strike feature of fatigue failure is that unlike other types of failure it can happen even when the applied cyclic stress is less than yield stress of the mechanical parts.

Many researchers have investigated different approaches regarding fatigue life prediction for metals, for example [3]-[5]. A review article presented by [6] reviews fatigue life prediction techniques for metallic materials and it concluded that the ideal fatigue life prediction model has to involve the main features of those already established methods. In some practical applications, many mechanical parts and systems are subjected to a mixed mode loading conditions represented by torsion and cycling bending [7]. This kind of loading has a significant effect on fatigue behavior and fatigue life prediction of those parts. Therefore, the experimental investigation work in this paper is designed to tackle this issue.

1.1 Fatigue Life Estimation

Fatigue life estimation for mechanical parts and structures is often obtained through conducting experimental tests on specimens from same metal subjected to same loading. Consequently, fatigue life curve which is called stress- cycles to failure (S-N) curve can be constructed by testing specimens under constant amplitude loading. The mathematical expression of this curve is usually given as [2]:

$$\sigma_f = A\, N_f^{\ \alpha} \qquad (1)$$

where σ_f is the applied cyclic stress, N_f number of cycles till to failure. The two constants A and α can be found experimentally.

A typical S-N curve is shown in Figure (1). In this figure, two types of curves are given corresponding to two types of materials namely; ferrous and non-ferrous metals. Ferrous metals have a fatigue limit or endurance limit which represents a stress level below which the material does not fail and can be cycled infinitely as illustrated in curve A. Non-ferrous metals and alloys, such as aluminum, magnesium, and copper alloys, do not have well-defined endurance limits. These materials instead show a continuous decrease in number of cycle to failure as indicated in curve B. In such cases a fatigue strength S_f for a given number of cycles must be identified. An effective endurance limit for these materials is usually defined as the stress that causes failure at $1x10^8$ loading cycles [1].

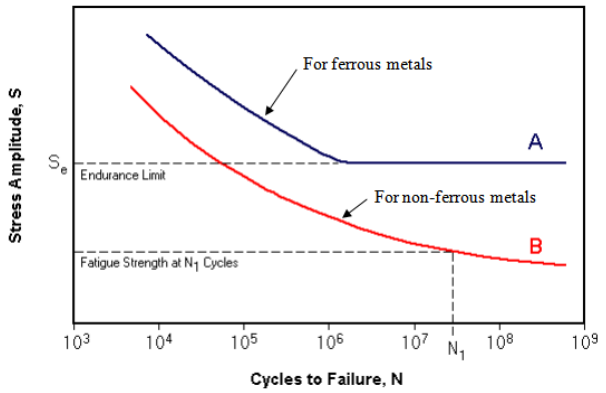

Figure 1: A typical S-N Curve.

1.2. Cumulative fatigue damage

In 1945, Miner [8] first expressed the concept of cumulative fatigue damage in a mathematical form as:

$$D = \sum(n_i / N_{fi}) \quad (2)$$

where D denotes the damage, and n_i and N_{fi}, are the applied cycles and the total cycles to failure under ith constant-amplitude loading level respectively. A comprehensive review of cumulative fatigue damage theories for metals and their alloys, emphasizing the approaches developed between the early 1970s to the early 1990s is provided by [9].

2. Experimental Work

This section presents the experimental part done in this paper. That involves, metals used; their mechanical properties and chemical composition, fatigue test machine, fatigue test specimen, application of prior torsion and the fatigue tests implemented.

2.1 Metals Used

Two types of metals have been used in this work. The first one is 2024-T4 aluminum alloy which has a wide range of application in aircrafts industry and aerospace. The second one is 304L (Austenitic Stainless Steel) which has an important role in industry. Tables (1) and (2) show the chemical compositions for 2024-T4 aluminum alloy and 304L steel alloy respectively [10], [11]. The standard and the measured values are both presented in these tables. It can be seen from the values indicated in these tables that the measured values are within the permitted percentage for both alloys used in this paper.

Table 1: Chemical composition for (2024-T4).

Element	Si	Cu	Mn	Mg	Fe	Zn	Cr	Ti	Al
Standard Value Wt %	0.5-1.2	3.9-5.0	0.4-1.2	0.2-0.8	0.7	0.25	0.1	0.15	Rem
Measured Value Wt%	0.79	4.34	0.83	0.55	0.58	0.19	0.06	0.09	Rem

Table 2: Chemical composition for 304L steel alloy

Element	C	Mn	Cr	Ni	Mo	Fe
Standard Value Wt %	0.03	2.0	18-20	8-12	-	Rest
Measured Value Wt%	0.025	1.63	18.8	10.2	0.03	Rest

The tensile test and the hardness test were implemented to determine the mechanical properties for both metals used in this study. Tables (3) and (4) show the standard mechanical properties and the measured ones for 2024-T4 and 304L respectively. Figure (2) shows the tensile test specimen used for both metals.

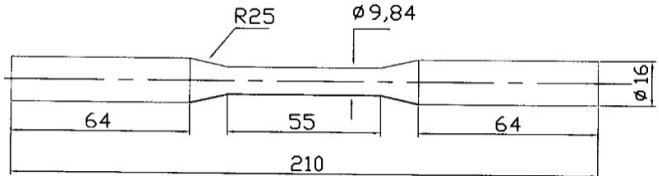

Figure 2: Tensile test specimen, dimensions are in mm.

Table 3: Mechanical properties for 2024-T4 alloy

	Yield strength N/mm²	Tensile Strength N/mm²	Elongation %	Hardness	
				HRB	HB
Standard Value	290	427	20	65-73	105
Measured Value	284	414	18,2	69	103

Table 4: The mechanical properties for 304L alloy.

	Yield strength N/mm²	Tensile Strength N/mm²	Elongation %	Hardness	
				HRB	HB
Standard Value	269	558	55	90-99	150
Measured Value	260	549	51.6	98.7	144

2.2 Rotating Fatigue Test Machine

The rotating bending fatigue test machine (HSM 19 HI-TECH) shown in Figure (3) has been utilized to implement both constant and variable amplitude fatigue tests. This rig works at frequency of 2800 rpm imposing cyclic bending stress in a sine wave fashion which has constant amplitude and zero mean stress. The value of stress ratio is (R = -1). The load is applied perpendicularly on the specimen axis producing bending moment and consequently the surface of the specimen will be subjected to tension-compression stresses when it rotates. The required load for a given stress magnitude can be determined by considering the specimen as a cantilever beam as indicated in the following expression:

$$P = \sigma * \pi d^3 /125.7 *32 \quad (3)$$

where (P) is the required load to apply for a given stress (σ) while (d) represents the minimum diameter of the specimen measured in mm. The distance from this point to the line action of the applied load is (125.7 mm). The rig is provided

with a counter to calculate number of cycles till to specimen failure. This counter has a micro switch that stops it automatically when the specimen breaks. The test specimen is fixed between two grips in the rig as shown in Figure (3), where (1) is the circuit break, (2) is fatigue test specimen, (3) is electrical motor, (4) is power unit and (5) is the rig jaws.

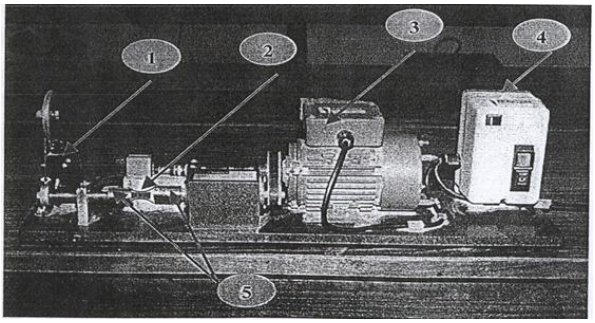

Figure 3: A: Fatigue test machine.

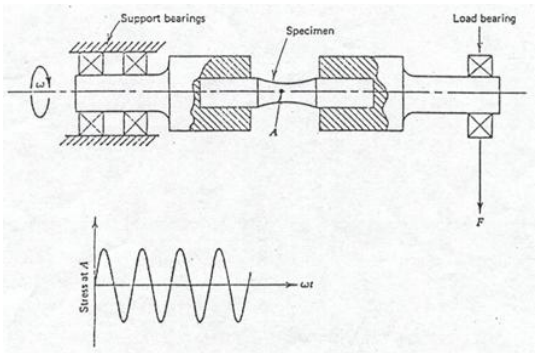

Figure 3: B: Working diagram for the fatigue test machine.

2.3 Machining Fatigue Test Specimen

The fatigue test specimens have been machined according to the standard specifications of the fatigue test rig used in this work (HSM, 19 Rotating fatigue machine). Figure (4) shows the machined fatigue test specimen. The curvature area (R20) has been polished according to the standard procedure [10].

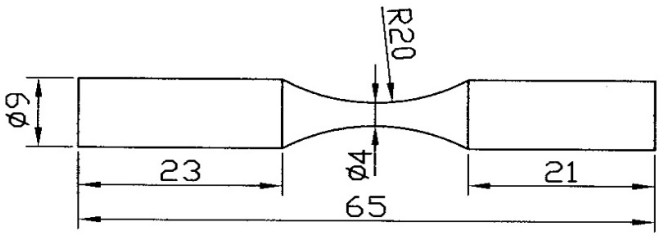

Figure 4: Fatigue test specimen.

The surface roughness of the specimens has been measured using Perthometer 510D device which has a probe type (Perthometer PMK). Table (5) shows typical results for the surface roughness measured.

Table 5: Surface roughness measured for 8 specimens.

Average Roughness Ra(μm)	0.21	0.17	0.2	0.14	0.2	0.13	0.19	0.15
MaximumPeak Rmax. (μm)	1.17	1.24	2.12	1.68	1.5	1.27	1.22	1.51

2.4 Applying Prior Torsion

A torsion test rig has been utilized to apply prior torsion on fatigue test specimens before subject them to fatigue tests. This rig is provided with a counter for the imposing torque resulting from applying a given angle of twist. A prior torsion of (2^0) was applied on (26) specimens and these specimens have then been used as in below:

1-(20) Specimens (10 specimens from 2024-T4 and 10 specimens from 304L) to perform constant amplitude loading tests to construct the S-N curves under mixed mode loading.
2-(6) Specimens from 304L alloy tested under cumulative fatigue damage.

Table (6) shows the results from applying prior torsion of 2^0 and the recorded torsional moment (torque) on the two types of metals used. These specimens were then used in constant amplitude fatigue test. Table (7) presents the results of applying prior torsion on specimens from 304L alloy and the resulting torsional moment. These specimens were then used for implementing cumulative fatigue damage.

Table 6: Results of applying prior torsion of 2^0 on both type of specimens for constant amplitude fatigue test.

304L specimen No.	Resulting torsional moment (T) (N.m)	2024-T4 specimen No.	Resulting torsional moment (T) (N.m)
1SP	2.50	1AP	1.80
2SP	2.30	2AP	1.90
3SP	2.60	3AP	1.80
4SP	2.50	4AP	2.00
5SP	2.50	5AP	1.98
6SP	2.30	6AP	1.80
7SP	2.50	7AP	2.00
8SP	2.60	8AP	2.00
9SP	2.30	9AP	1.96
10SP	2.50	10AP	1.80

Table 7: Results of applying prior torsion (2^0) on 304L specimens for cumulative fatigue damage.

Specimen No.	Resulting torsional moment (T) in N.m
6SC	1.91
7SC	2.00
8SC	1.80
9SC	1.90
10SC	1.79
11SC	1.94

2.5 Implementing constant amplitude loading test

This test has been implemented on (40) specimens divided into (4) groups through which four S-N curves have been constructed. The first group (A) involves (10) Specimens from (2024-T4) Al alloy without prior torsion, the second group (B) includes (10) specimens from (2024-T4) subjected to prior torsion, the third group (C) has (10) specimens from (304L) alloy without prior torsion and the fourth group (D)

involves (10) specimens from (304L) alloy with prior torsion. All these specimens have been tested under rotating bending fatigue. The experimental results for groups (A) and (B) are presented in Table (8) and Table (9) respectively.

Table 8: Experimental results under constant amplitude test for 2024-T4 alloy

Specimen No.	Applied stress (Mpa)	No. of cycles to failure, N_f
1A	300	38000
2A	300	34200
3A	250	192000
4A	250	110000
5A	200	890000
6A	200	1420000
7A	150	8440000
8A	150	7600000
9A	120	11820000
10A	120	12440000

Table 9: Experimental results under mixed mode loading test (with prior torsion of 2^0) for 2024-T4 alloy

Specimen No.	Applied stress (Mpa)	No. of cycles to failure, N_f
1AP	300	72200
2AP	300	68100
3AP	250	284000
4AP	250	240000
5AP	200	1610000
6AP	200	1830000
7AP	150	9920000
8AP	150	10110000
9AP	120	14990000
10AP	120	16420000

The results shown in Table (8) and Table (9) have then been used to construct the S-N curves for the 2024-T4 alloy with and without prior torsion as shown in Figure (5). These two curves can be expressed mathematically by the following:

$$\sigma_f = 1399.4\ N_f^{-0.144} \quad \text{(without prior torsion)} \qquad (4)$$

$$\sigma_f = 1788.8\ N_f^{-0.157} \quad \text{(with prior torsion)} \qquad (5)$$

where σ_f is the alternative stress at the failure (N/mm^2), N_f denotes number of cycles till to failure. The endurance limit for this alloy has been determined with and without prior torsion from these two S-N curves to be around (138 N/mm^2) at 10^7 cycle and (142 N/mm^2) at 10^7 cycle respectively.

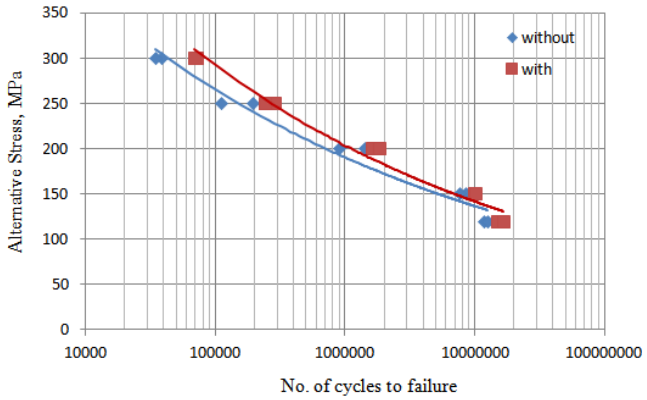

Figure 5: S-N curve for 2024-T4 with and without prior torsion.

The experimental results for groups (C) and (D) are indicated in Table (10) and Table (11) respectively.

Table 10: Experimental results under constant amplitude test for 304L alloy.

Specimen No.	Applied stress (Mpa)	No. of cycles to failure, N_f
1S	450	10200
2S	450	11700
3S	400	46300
4S	400	62100
5S	350	145200
6S	350	186700
7S	300	2120000
8S	300	2362000
9S	250	10 000000*
10S	250	10 000000 *

* Refers to unbroken specimen till to 10^7 cycle.

Table 11: Experimental results under mixed mode loading test (with prior torsion of 2^0) for 304L alloy

Specimen No.	Applied stress (Mpa)	No. of cycles to failure, N_f
1SP	450	1800
2SP	450	1600
3SP	400	37600
4SP	400	42800
5SP	350	86400
6SP	350	122600
7SP	300	1882000
8SP	300	1781000
9SP	250	10 000000 *
10SP	250	10 000000 *

Refers to unbroken specimen till to 10^7 cycle.*

The results indicated in Tables (10) and (11) have then been utilized to construct the S-N curves for 304L alloy with and without prior torsion as shown in Figure (6). These two curves can be expressed mathematically by the following:

$$\sigma_f = 977.15\ N_f^{-0.083} \quad \text{(without prior torsion)} \qquad (6)$$

$\sigma_f = 780.37\ N_f^{-0.069}$ (with prior torsion) (7)

The endurance limit for this alloy has been determined with and without prior torsion from these two S-N curves to be around (260 N/mm^2) at 10^7 cycle and (273 N/mm^2) at 10^7 cycle respectively.

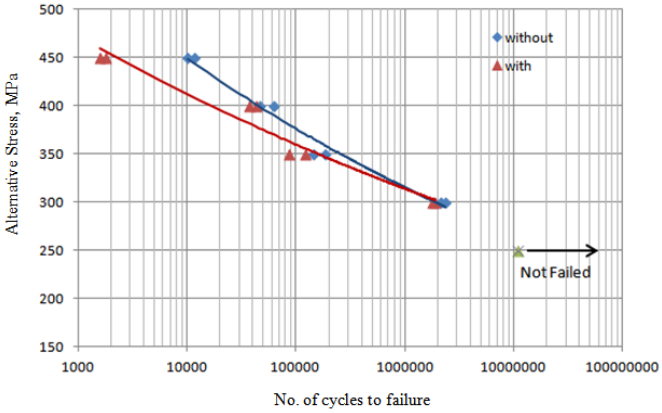

Figure 6: S-N curve for 304L steel alloy with and without prior torsion

2.6 Implementing variable amplitude loading test

This test was implemented on (13) specimens of (304L) steel alloy divided into 4 groups which have been subjected to cumulative fatigue damage tests resulting from applying variable amplitude loading according to (Low-High) loading test program with a constant number of cycles (10000 cycles) for each applied stress level in the experimental test program as detailed in the following:

Group A: (5) Specimens subjected to (Low-High) loading program were tested under rotating bending for different values for high and low stresses as indicated in Figures (7), (8), (9), (10) and (11). *Group B:* (4) specimens subjected to (Low-High) loading program were tested under mixed mode loading (rotating bending and prior torsion of (2^0) for the same different values for high and low stresses as indicated in Figures above. *Group C:* (2) Specimens subjected to Block Test Loading program were tested under rotating bending for different values for high stress as indicated in Figures (12) and (13). *Group D:* (2) Specimens subjected to Block Test Loading program were tested under mixed mode loading for different values for high stress as indicated in Figures (12) and (13).

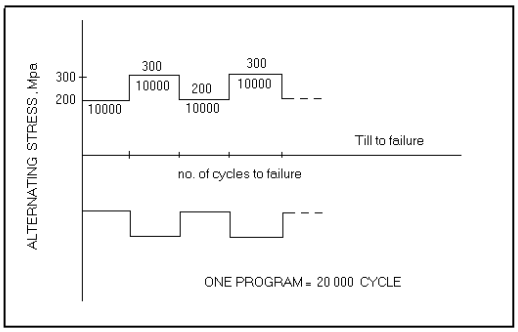

Figure 7: Experimental loading test program type low-High for stress range (200-300) Mpa

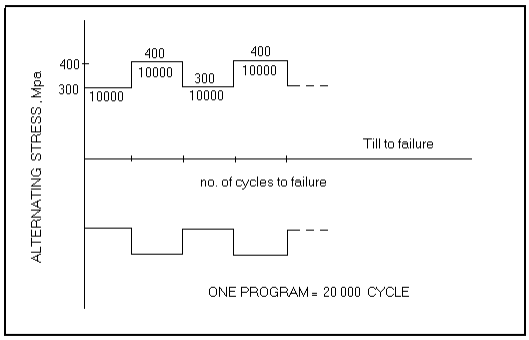

Figure 8: Experimental loading test program type Low-High for stress range (300-400) Mpa

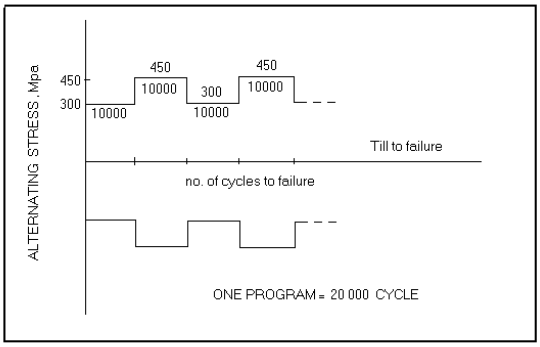

Figure 9: Experimental loading test program type Low-High for stress range (300-450) Mpa.

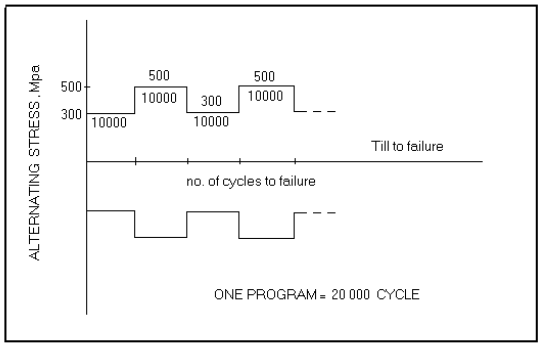

Figure 10: Experimental loading test program type Low-High for stress range (300-500) Mpa

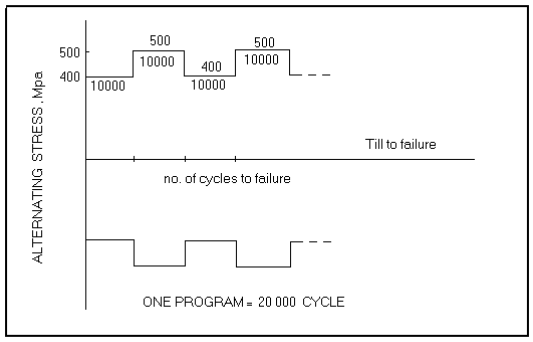

Figure 11: Experimental loading test program type Low-High for stress range (400-500) Mpa

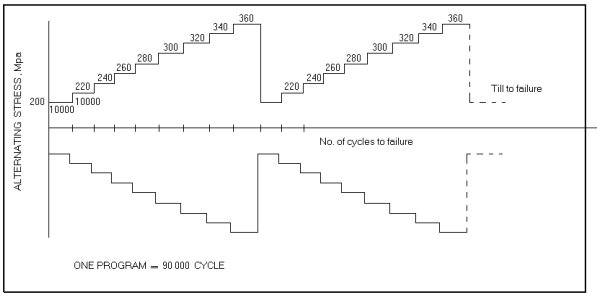

Figure 12: Experimental loading test program type Block-Loading Test for stress range (200-360) Mpa

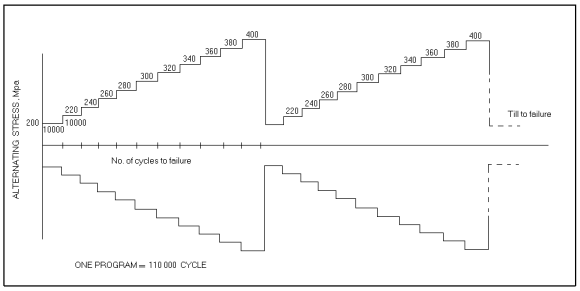

Figure 13: Experimental loading test program type (Block-Loading Test) for stress range (200-400) Mpa

The experimental results obtained for groups (A) and (B) are indicated in Tables (12) and (13) respectively. The comparison with the fatigue life prediction using Miner is also shown in these two tables.

Table 12: Fatigue life of 304L alloy under cyclic bending

Specimen No.	Applied stress, (Mpa)	No. of test programs	Experimental damage rule $D_{exp.}$	Miner's Damage ratio D_{miner}	No. of programs according to Miner rule
2S	300 – 400	64.7	14.548	1	4.448
3S	300 – 450	2.56	2.608	1	0.982
4S	300 – 500	0.895	3.570	1	0.250
5S	400 – 500	0.805	3.383	1	0.237

Table 13: Fatigue life of 304L alloy under mixed mode loading

Specimen No.	Applied stress, (Mpa)	No. of test programs	Experimental damage rule $D_{exp.}$	Miner's Damage ratio D_{miner}	No. of programs according to Miner rule
6SC	300 – 400	15.1	9.141	1	1.652
7SC	300 – 450	1.795	7.864	1	0.228
8SC	300 – 500	0.630	16.282	1	0.038
9SC	400 – 500	0.560	27.00	1	0.0207

Tables (14) and (15) show the experimental results obtained for groups (C) and (D) respectively. The comparison with Miner's rule results are also given in these two tables.

Table 14: Fatigue life of 304L alloy under cyclic bending according to loading program of type Block Test

Specimen No.	Applied stress in loading program, (Mpa)	No. of test program	Experimental damage rule D_{exp}	Miner's Damage ratio D_{miner}	No. of programs according to Miner rule
10SB	200 – 360	17.957	1.853	1	9.688
11SB	200 – 400	2.894	1.101	1	2.865

Table 15: Fatigue life of 304L alloy under mixed mode loading according to loading program of type Block Test.

Specimen No.	Applied stress in loading program, (Mpa)	No. of test program	Experimental damage rule D_{exp}	Miner's Damage ratio D_{miner}	No. of programs according to Miner rule
12S	200 – 360	27.7	4.463	1	6.206
13S	200 – 400	6.942	7.043	1	0.985

3. Discussion

The experimental results obtained in this work show that the mixed mode loading has a remarkable effect on the fatigue life predictions under both constant and variable amplitude loading tests. This effect was manifested in changing the fatigue life represented in number of cycle till to failure.

As far as the results of constant amplitude loading are concerned, it can be deduced by comparing results from group A with that from group B that there is an increase in fatigue life of 2024-T4 under mixed mode loading. The justification for that increase in fatigue life is that the prior torsion (2^0) enhanced the internal strain energy of the alloy which then becomes in unstable condition. The amount of strain energy stored in the metal depends on the degree of cold working (prior torsion). This extra energy is not distributed regularly throughout the material but it is concentrated at some point creating an increase in its energy level. During rest period, when the torsion is released, several resisting walls will be created due to this energy which resists cracks initiation and their propagation. Therefore, the speed of short cracks become very slow and consequently enhances fatigue life of the component [2]. Figure (5) shows the S-N curve of 2024-T4 alloy using both type of loading. It can be seen from these two curves that the fatigue life is increased as a result of imposing mixed mode loading. In addition, the endurance limit of this alloy has been increased from (138 Mpa) to (142.4 Mpa) as a result of applying prior torsion.

Comparing results of groups C and D and by noticing Figure (6) which shows the fatigue life curve of 304L alloy, we find that the fatigue limit which was around 273 Mpa, has decreased to 260 Mpa due to the passive effect of prior torsion on this metal. This reduction in fatigue life of the specimens enables the designer to consider extra safety factors in estimating components fatigue life [1].

Regarding the results obtained for variable amplitude loading tests, the results of the 4 groups represent fatigue life predictions of specimens from 304L alloy subjected to cumulative fatigue damage resulting from the fact that many mechanical components and systems are in practice subject to combined loading, torsion and cyclic bending.

The change in fatigue life value can be expressed in a fatigue life ratio (β) as in the following:

$\beta_1 =$ N_f (with prior torsion of 2^0) / N_f (without prior torsion)

Table (16) shows the effect of applied stress ranges on the fatigue life ratios, β_1 for the Low-High loading program while Table (17) indicates the effect of mixed mode with

prior torsion of 2^0 on the fatigue life ratio β_1 subjected to Block-Test loading program.

Table 16: Effect of applied stress range on fatigue life ratio under Low-High loading program

Applied stresses range, Mpa	Fatigue life ratio, β_1
300 – 400	0.233
300 – 450	0.701
300 – 500	0.704
400 – 500	0.764

Table 17: Effect of mixed mode with prior torsion of 2^0 on fatigue ratio subjected to Block-Test loading program

Applied stresses range, Mpa	Fatigue life ratio, β_1
200 – 360	1.543
200 – 400	2.398

Comparing results from first and second groups we notice that there is a reduction in fatigue life due to the effect of prior torsion (2^o) for different stress ranges in loading program. The amount of reduction in (β_1) varies with variation in the range of high applied stress range and as the amplitude of high stress increases, the fatigue life ratio (β_1) increased. The reason for that is when the high stress increases the time period of the effect of prior stress resulting from applying torsional moment will decrease. Consequently, the fatigue life of the components will be reduced.

4. Conclusions

In this work, the effect of mixed mode loading on fatigue life prediction of structural metals has been investigated experimentally. Both constant and variable amplitude loading tests have been implemented. Consequently, the S-N curves of these two alloys have been constructed with and without introducing mixed mode loading. These curves can be utilized to predict fatigue behavior under constant amplitude loading.

The results obtained in this study show that imposing mixed mode loading (with prior torsion 2^0) has been resulting in increasing fatigue lives of 2024-T4 aluminum alloy as a result of occurring strain hardening phenomenon which increases crack propagation strength and consequentially increase fatigue life while for 304L steel alloy, fatigue lives decrease due to imposing pre-stresses resulting from applying torsional moment. The experimental damage ratio ($D_{exp.}$) for the implemented tests was greater than (1). Therefore, fatigue life predictions were safe according to Miner rule.

References

[1] J. Schijve, Fatigue of Structures and Materials, second edition, Springer Science & Business Media, 2009.
[2] R. I. Stephens, A. Fatemi, R. Stephens, and H. O. Fuchs, Metal Fatigue in Engineering, John Wiley & Sons, New York, NY, USA, 2000.
[3] Ge. Jingran, Yi Sun, Jun Xu, Zhiqiang Yang, Jun Liang, Fatigue life prediction of metal structures subjected to combined thermal-acoustic loadings using a new critical plane model, International Journal of Fatigue, Volume 96, March 2017, Pages 89–101.
[4] J.F. Durodola, N. Li, S. Ramachandra, A.N. Thite. A pattern recognition artificial neural network method for random fatigue loading life prediction, International Journal of Fatigue, Volume 99, Part 1, June 2017, Pages 55–67.
[5] M. Makkonen, "Predicting the total fatigue life in metals," International Journal of Fatigue, vol. 31, no. 7, pp. 1163–1175, 2009.
[6] E. Santecchia, A. M. S. Hamouda, F. Musharavati, E. Zalnezhad, M. Cabibbo, M. El Mehtedi, and S. Spigarelli. A Review on Fatigue Life Prediction Methods for Metals. Advances in Materials Science and Engineering, 2016.
[7] J. Schijve, Fatigue of Structures and Materials, Springer Science & Business Media, 2001.
[8] M. A. Miner, "Cumulative damage in fatigue," Journal of Applied Mechanics, vol. 12, pp. A159–A164, 1945.
[9] A. Fatemi, L. Yang, "Cumulative fatigue damage and life prediction theories: a survey of the state of the art for homogeneous materials", International Journal of Fatigue, Volume 20, issue 1, 1998, pages 9-34.
[10] ASM Handbook Volume 2: Properties and Selection: Nonferrous Alloys and Special-Purpose Materials. 1990.
[11] Donald Peckner and Irving Melvin Bernstein, Handbook of stainless steels, McGraw-Hill, 1977.

Author Profile

Saad S. Al-Khfaji received the B.S., M.Sc. and PhD degrees in Mechanical Engineering from Baghdad University, University of Technology and the University of Nottingham UK, in 1993, 1999 and 2012, respectively. During 2012-2015, he worked at the Ministry of Science and Technology, Iraq. He now with the Ministry of Higher Education and Scientific Research, Baghdad.